[CANCER RESEARCH Vol. 62, 1966–1970, April 1, 2002

Metabolic Markers of Breast Cancer: Enhanced Choline Metabolism and Reduced Choline-Ether-Phospholipid Synthesis[1]

Rachel Katz-Brull,[2, 3] Dalia Seger, Dalia Rivenson-Segal, Edna Rushkin, and Hadassa Degani

Department of Biological Regulation, Weizmann Institute of Science, Rehovot 76100, Israel

ABSTRACT

Specific genetic alterations during malignant transformation may induce the synthesis and breakdown of choline phospholipids, mediating transduction of mitogenic signals. The high level of water-soluble choline metabolites in cancerous breast tumors, relative to benign lesions and normal breast tissue, has been used as a diagnostic marker of malignancy. To unravel the biochemical pathways underlying this phenomenon, we used tracer kinetics and ^{13}C and ^{31}P magnetic resonance spectroscopy to compare choline transport, routing, and metabolism to phospholipids in primary cultures of human mammary epithelial cells and in MCF7 human breast cancer cells. The rate of choline transport under physiological choline concentrations was 2-fold higher in the cancer cells. The phosphorylation of choline to phosphocholine and oxidation of choline to betaine yielded 10-fold higher levels of these metabolites in the cancer cells. However, additional incorporation of choline to phosphatidylcholine was similar in both cell types. Thus, enhanced choline transport and augmented synthesis of phosphocholine and betaine are dominant pathways responsible for the elevated presence of choline metabolites in cancerous breast tumors. Uniquely, reduced levels and synthesis of a choline-ether-phospholipid may also serve as a metabolic marker of breast cancer.

INTRODUCTION

Elevated concentrations of choline and choline metabolites (composite choline) were observed by MRS[4] in a variety of malignancies (1, 2). This elevation has been particularly useful for differentiating between malignant and benign breast lesions, because the former contain a significantly higher level of composite choline than the latter (3–8). However, to fully exploit the diagnostic potential of breast MRS, it is necessary to elucidate the underlying biochemical mechanisms leading to this metabolic phenomenon.

Choline, a quaternary amine, is an essential nutrient supplied predominantly by the diet (9, 10). The capacity to take up and secrete high levels of choline and choline metabolites is a central function of mammary epithelial cells. During lactation, these cells are capable of concentrating choline from the plasma and, subsequently, secreting milk that is rich in choline-containing metabolites, primarily PCho and GPCho (11).

Active transport and diffusion are major mechanisms in the uptake of choline across cellular membranes. The diffusion capacity through membranes is related to the composition and special assembly of lipids, predominantly phospholipids and cholesterol, as well as of proteins. Routing of choline through its various metabolic pathways is cell and tissue specific (12). The intracellular metabolism of choline in the breast is partitioned among two major pathways: (*a*) synthesis of PtdCho; and (*b*) oxidation to produce the methyl donor betaine.

Choline metabolism and choline-derived metabolites can undergo extensive alterations as a result of malignant transformations. Progression of HMECs from a normal to a malignant phenotype was shown recently to be associated with a reversal in the ratio of PCho to GPCho, as well as an overall increase in the content of these two metabolites (13).

PCho is a precursor of choline-derived phospholipids, as well as a product of their hydrolysis. The synthesis and degradation of phospholipids may be induced by growth factors that play a major role in malignant transformations (14, 15). The level of PCho in human breast cancer cells was found to be ~10-fold higher than in HMECs (13, 16, 17). Moreover, high levels of PCho and other phosphomonoesters were detected in human breast cancer biopsies and in patients *in vivo* (1, 18). The high levels of PCho correlated with up-regulation and increased activity of choline kinase, and choline kinase inhibitors exhibited antitumor activity (19, 20). High choline transport was suggested as the cause for the elevated levels of PCho in breast cancer (21). However, the exact role of PCho in malignant transformation and the involvement of other choline metabolites in this transformation are not well understood.

We present herein comparative studies of the metabolic steps that determine the nature and distribution of choline metabolites in normal and cancerous mammary epithelial cells. Detailed radioactive tracer measurements and model-based analyses yielded the mechanisms and kinetic parameters of choline transport. Additional metabolic studies using ^{13}C- and ^{31}P-MRS and ^{13}C-labeled choline enabled us to monitor the synthesis of PCho and betaine and characterize the composition and turnover of choline-derived phospholipids. Our results demonstrated enhanced transport of choline, augmented synthesis of PCho and betaine, and suppression of the synthesis of choline-derived ether lipids in breast cancer cells.

MATERIALS AND METHODS

Tissue Culture. MCF7 human breast cancer cells were cultured routinely in DMEM supplemented with 6% FCS and antibiotics, as described previously (21). T47D-clone 11 human breast cancer cells were routinely cultured in RPMI 1640 supplemented with 10% FCS, as described previously (17). Both media contained 28 μM choline, with an additional ~2 μM choline from the serum.

Primary cultures of HMECs were obtained from two sources: Clonetics Corp., San Diego, CA, which provided HMECs isolated from epithelial organoids of human breast tissue; and our laboratory. The cells from Clonetics were cultured in serum-free mammary epithelial cell growth medium supplemented with bovine pituitary extract, insulin, human epidermal growth factor, hydrocortisone, and antibiotics. For the second source of HMECs (HMEC*s), we isolated, separated, and cultivated the cells in our laboratory by processing breast tissue obtained from mammoplastic reduction surgery, as described previously (17).

Choline Transport. MCF7 and HMEC cells were preincubated for 3 h in choline-free DMEM supplemented with 2% FCS. Transport experiments were initiated by adding various concentrations of choline (1–400 μM) to the above medium and trace amounts (1–2 μCi) of [*methyl*-^{14}C]choline chloride (Sigma

Received 8/24/01; accepted 1/23/02.

The costs of publication of this article were defrayed in part by the payment of page charges. This article must therefore be hereby marked *advertisement* in accordance with 18 U.S.C. Section 1734 solely to indicate this fact.

[1] This work was supported by the Israel Science Foundation and The Susan G. Komen Breast Cancer Foundation. H. D. is the incumbent of the Fred and Andrea Fallek Professorial Chair for Breast Cancer Research and heads the Willner Family Center for Vascular Biology.

[2] To whom requests for reprints should be addressed, at Center for Advanced Imaging, W/CC-090, Beth Israel Deaconess Medical Center, One Deaconess Road, Boston, MA 02215. Phone: (617) 754-2009; Fax: (617) 754-2010; E-mail: rkatzbr@caregroup.harvard.edu.

[3] Present address: Department of Radiology, Beth Israel Deaconess Medical Center Harvard Medical School, Boston, MA 02215.

[4] The abbreviations used are: MRS, magnetic resonance spectroscopy; PCho, phosphocholine; GPCho, glycerophosphocholine; PtdCho, phosphatidylcholine; HMEC, human mammary epithelial cell; NMR, nuclear magnetic resonance; NTP, nucleoside triphosphate.

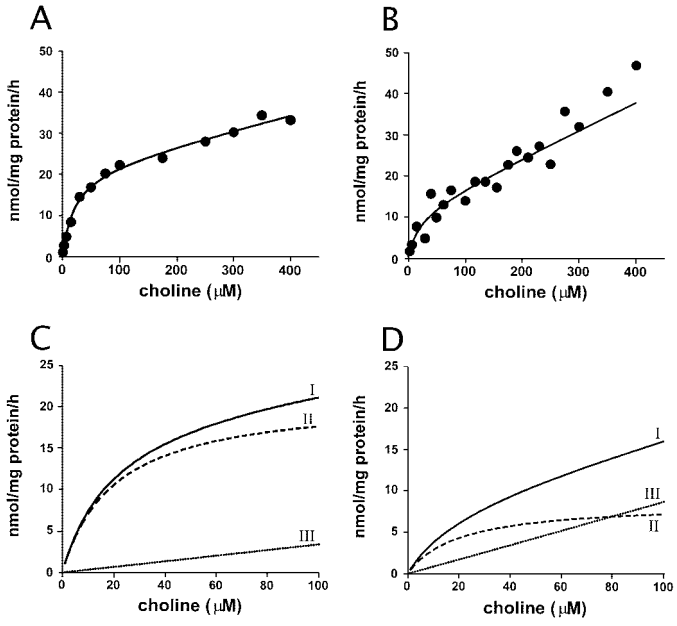

Fig. 1. Variation in the initial rate of choline transport with choline concentration in MCF7 cells and HMECs. The *solid lines* in *A* (MCF7 cells) and *B* (HMECs) demonstrate the best curve fitting to the kinetic equation: $\upsilon = V_{max}S/(K_m + S) + K_dS$. *C* and *D*, calculation of choline transport in MCF7 and HMECs, respectively, at 0–100 μM choline, using the transport rate constants described in Table 1. *I*, initial rate of choline uptake (equation above); *II*, saturable choline uptake; *III*, passive diffusion of choline.

Chemical Co., St. Louis, MO). For each choline concentration, samples were incubated with the tracer at 36°C for 4, 8, and 12 min. After we cooled the samples to 0°C, they were washed three times with ice-cold PBS, and the cells were scraped with ice-cold methanol and mixed with scintillation fluid for additional β-counting. The initial transport rates were obtained by a linear fitting of the amount of extracted radioactive choline at 4, 8, and 12 min (per cell number). The initial transport rates were further normalized to mg protein/cell, independently determined by the Bradford method (22), yielding a value of 220 ± 8 picogram/cell for MCF7 cells and 410 ± 50 picogram/cell for HMECs. The ~2-fold higher protein content of HMECs, as well as the 2-fold higher NTP (predominantly ATP) correlated with the larger volume of the latter cells (17).

The kinetic parameters were calculated using Stein's method for zero-*trans* transport (23). The mechanism(s) of transport was revealed through specific patterns of the plots of the initial rate υ *versus* choline concentration *S*, υ/S (*k*) *versus S*, and $1/k$ *versus S*. The kinetic parameters were calculated by a nonlinear fitting of each mode of plotting and are presented as the mean ± SD of the three plots.

Choline Metabolism. MCF7 cells and HMECs ($1.5–2 \times 10^8$ and $2–4 \times 10^7$ cells, respectively) were incubated at 36°C for 24 h in choline-free culture medium supplemented with 100 μM [1,2-^{13}C]choline, 99% ^{13}C enriched (Cambridge Isotope, Ltd., Andover, MA). The medium was then collected, and the cells were extracted using the dual-phase extraction method (24).

The methanol-water phase was treated with Chelex-100 (Sigma), lyophilized to dryness and kept at −20°C. Before the NMR measurement, the dried residue was redissolved in 0.5 ml of D_2O (99.9% enriched; Cambridge Isotopes, Ltd.) containing 5 μl of methanol as a standard for ^{13}C measurements, at a pH of 8–8.3. After recording the ^{13}C spectra and before the ^{31}P measurements, 10 mM EDTA was added to the samples. The chloroform of the lipid phase was evaporated under N_2, and the dried residue was redissolved in a mixture of 0.4 ml of chloroform and 0.2 ml of methanolic EDTA solution (25).

The large volumes of the culture medium were concentrated by sequential lyophilizations. The resulting dried residue was dissolved in 0.5 ml of D_2O (99.9% enriched; Cambridge Isotopes).

Lipid extraction of T47D and the second source of HMEC*s was performed using a modification of Folch's method, which extracted phospholipids with an efficiency similar to that of the dual-phase extraction method described above (24).

NMR Spectroscopy. High-resolution NMR spectra were recorded on a DMX-500 spectrometer operating at 11.7 Tesla (Bruker Analytic GMBH, Karlsruhe, Germany). ^{13}C spectra of the water-soluble metabolites and the lipids were recorded at 125.7 MHz, using a ^{1}H/^{13}C dual probe and applying 60° pulses, 2.4-s repetition time, and continuous composite pulse proton decoupling. ^{31}P NMR spectra of the water-soluble metabolites and the lipids were recorded at 202.4 MHz by applying 45° pulses, a repetition time of 2 s, and continuous composite pulse proton decoupling. The signals of α-NTP (at −10.03 ppm) and the signal of added phenylphosphonic acid served as references for chemical shift and concentration, respectively. Signal intensity and area in NMR spectra were measured with XWIN-NMR (Bruker Biospin MRI GMBH). The amount of NTP was determined from the combined area of γ-NTP + β-nucleoside diphosphate. The nonphosphorylated metabolites were referenced to NTP through the use of the PCho signal, which appeared in both the ^{13}C and the ^{31}P spectra. The areas of the signals in both the ^{31}P and the ^{13}C spectra were converted to concentration units, percent enrichment, or metabolite ratio, taking into account ^{13}C enrichment as well as differences attributable to relaxation and nuclear Overhauser enhancement. The final results are presented as the mean ± SE.

RESULTS

Choline Transport

The mechanisms contributing to choline transport into MCF7 human breast cancer cells and HMECs, as well as the rate constants associated with each mechanism, were determined by applying a tracer kinetic method. The initial rate of choline uptake (υ) was measured as a function of choline concentration in the medium (*S*). Plots of υ *versus S* (Fig. 1, *A* and *B*) as well as υ/S and S/υ *versus S* revealed the presence of a saturable, Michaelis-Menten-like mechanism as well as a diffusion mechanism, according to: $\upsilon = V_{max}S/(K_m + S) + K_dS$, where K_m and V_{max} define the rate constant and maximum rate of the saturable transport, and K_d the diffusion rate constant. Fitting the data according to the above equation (Fig. 1, *A* and *B*) yielded similar K_ms in both MCF7 cells and HMECs (20 ± 5 μM and 14 ± 9 μM, respectively); however, V_{max} was 2-fold faster in the cancer cells (Table 1). Thus, MCF7 breast cancer cells exhibited increased choline transport activity and stimulation of choline uptake in the physiological range (10–30 μM) of choline (Fig. 1, *C* and *D*). Interestingly, the diffusion rate constant K_d was higher in HMECs, indicating changes in cell membrane properties during malignant transformation. However, this mechanism contributed significantly to choline transport only at high concentrations of choline, much above the physiological range (Fig. 1, *C* and *D*).

Choline Metabolism

Choline Routing. Differential routing and incorporation of choline into intracellular water-soluble metabolites were investigated in MCF7 cells and HMECs. ^{13}C labeling of choline metabolites was monitored after incubation with 100 μM [1,2-^{13}C]choline (high above the K_m of choline transport). The two ^{13}C methylene signals of intracellular choline, PCho and betaine, were clearly observed in the ^{13}C spectra of the water phase extracts of MCF7 cells (Fig. 2*A*).

Table 1 *Kinetic parameters[a–e] of choline transport in HMECs and MCF7 cells*

	HMEC	MCF7
K_m (μM)	14 ± 9	20 ± 5
V_{max}[d] (nmol/mg protein/h)	8.8 ± 3.4	20 ± 4
K_d[e] (nmol/mg protein/h/μM)	83 ± 15	44 ± 19
R^2	0.94,[a] 0.86,[b] 0.84[c]	0.99[a,b,c]

[a–e] The saturable kinetic parameters, K_m and V_{max}, as well as the nonsaturable rate constant K_d, were determined by a nonlinear least squares curve fitting of: [a] initial rate, υ, *versus* choline concentration; S; [b] υ/S *versus S*; and [c] S/υ *versus S*. Results are presented as the mean ± SD of the values obtained in the three curve fittings. The corresponding values in units per cell are: [d] V_{max} of 3.6 ± 1.4 and 4.4 ± 0.8 fmol/cell/h in HMEC and MCF7, respectively; and [e] K_d of 34 ± 6 and 9.7 ± 4.1 fmol/cell/h/μM in HMEC and MCF7, respectively.

^{13}C-enriched betaine was also detected in the spectra of the concentrated incubation medium of these cells (Fig. 2*B*), indicating partial transfer of this metabolite to the medium. The ^{13}C spectra of HMECs demonstrated the presence of intracellular ^{13}C-enriched choline and PCho; however, betaine was not detected in the cell extracts or the medium.

In the spectra of both the normal and the cancer cells, we did not observe incorporation of the ^{13}C-enriched choline into GPCho, a breakdown product of PtdCho, indicating a slow turnover and breakdown of PtdCho. Both cell types were shown to contain GPCho, with the level in the cancer cells ~10-fold higher than in HMECs (17).

Quantitative analysis of the ^{13}C spectra showed that the pools of choline, PCho, and betaine were fully ^{13}C enriched in both cell types. However, the content of these metabolites was markedly different (Fig. 3). In MCF7 cells, most of the choline was metabolized to PCho, which accumulated in the cells to a very high level. The remaining choline was oxidized to betaine, but a large fraction of this metabolite (60%) was found in the medium. On the other hand, in HMECs most of the choline remained in its free form, and only a small fraction was metabolized to PCho, whereas oxidation to betaine was too low to be detected.

Choline Incorporation to Lipids. ^{31}P and ^{13}C NMR of lipid cell extracts monitored the incorporation of the ^{13}C-labeled choline into PtdCho and other choline-derived lipids. In the ^{31}P spectra of both the cancer and the normal cells, we observed signals of [1,2-^{13}C]-labeled PtdCho and signals at ^{13}C natural abundance of PtdCho, phosphatidylinositol, sphingomyelin, phosphatidylserine, phosphatidylethanolamine, phosphatidylethanolamine plasmalogen, and cardiolipin (Fig. 4 and Table 2). A distinct signal at 0.06 ppm downfield of PtdCho was detected in the spectra of HMECs (Fig. 4) and was not detected in

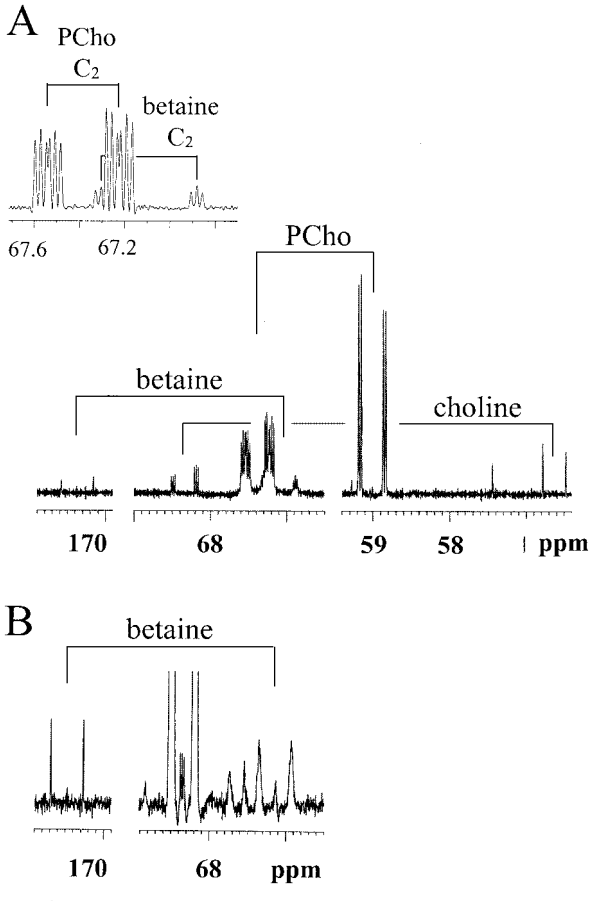

Fig. 2. ^{13}C spectra of intracellular water-soluble metabolites (*A*) and concentrated medium (*B*) of MCF7 cells. MCF7 cells were incubated with [1,2-^{13}C]choline as described in "Materials and Methods." The spectral regions demonstrate signals of [1,2-^{13}C]-labeled choline, PCho, and betaine. Each ^{13}C methylene signal of these three metabolites was split into two by the adjacent ^{13}C nucleus. The $^{13}C_2$ of choline, PCho, and betaine were further split by ^{14}N, whereas the $^{13}C_1$ and $^{13}C_2$ of PCho were split by ^{31}P. The other signals corresponded to other metabolites at ^{13}C natural abundance. The spectra were acquired with 25,500 scans (*A*) and 36,500 scans (*B*). *Inset* in *A*, expansion of the C_2 signals of both [1,2-^{13}C]PCho and [1,2-^{13}C]betaine.

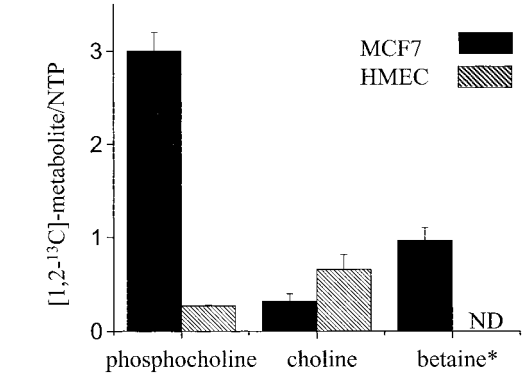

Fig. 3. Distribution of water-soluble ^{13}C-labeled choline and choline metabolites in MCF7 cells and HMECs. Cells were incubated with [1,2-^{13}C]choline as described in "Materials and Methods." Data were obtained from both ^{13}C and ^{31}P spectra. The results are presented as means; *bars*, SE. NTP per mg protein was similar in both cell types. *betaine**, total betaine (intracellular and released); *ND*, nondetectable level.

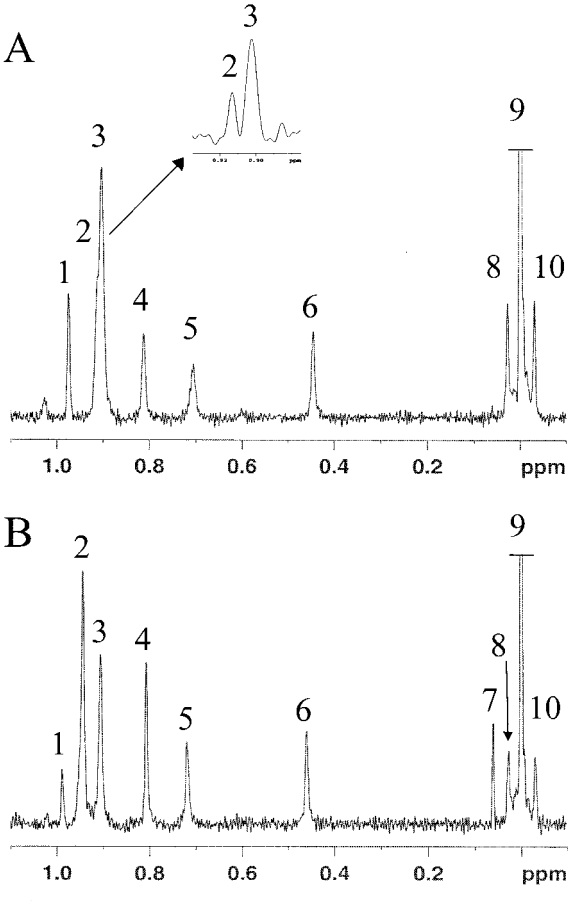

Fig. 4. ^{31}P spectra of the lipid phase of MCF7 and HMEC extracts. MCF7 cells (*A*) and HMECs (*B*) were incubated with [1,2-^{13}C]choline as described in "Materials and Methods." *Peak 1*, cardiolipin; *peak 2*, phosphatidylethanolamine-plasmalogen; *peak 3*, phosphatidylethanolamine; *peak 4*, phosphatidylserine; *peak 5*, sphingomyelin; *peak 6*, phosphatidylinositol; *peak 7*, choline-ether-phospholipid; *peaks 8* and *10*, [1,2-^{13}C]PtdCho; *peak 9*, PtdCho. *Inset* in *A*, expansion of phosphatidylethanolamine-plasmalogen and phosphatidylethanolamine region. The spectra were acquired with 48,100 scans (*A*) and 22,500 scans (*B*).

Table 2 *Phospholipid composition in HMEC and human breast cancer cells*

Results are presented as mean ± SE.

	PtdCho	PI[a]	SM + PS	PE	CL	Choline-ether-phospholipid	PE-plas
HMEC[b] $n = 6$	48.7 ± 1.4	6.0 ± 0.8	12.6 ± 1.3	11.4 ± 2.2	3.2 ± 0.8	4.4 ± 0.9	15.4 ± 0.6
MCF7 $n = 3$	54.3 ± 0.8	5.3 ± 0.3	8.9 ± 0.1	18.1 ± 0.8	5.7 ± 0.2	ND	7.8 ± 0.6[c]
T47D $n = 2$	65.6 ± 1.3	8.3 ± 0.4	7.4 ± 0.1	16.5 ± 0.1	2.3 ± 0.7	ND	ND

[a] PI, phosphatidylinositol; SM, sphingomyelin; PS, phosphatidylserine; PE, phosphatidylethanolamine; PE-plas, phosphatidylethanolamine-plasmalogen; CL, cardiolipin; ND, nondetectable level.

[b] HMEC ($n = 3$) and HMEC* ($n = 3$).

[c] Significant difference ($P = 0.001$, two-tail t test) between the HMECs and the MCF7 cells.

either MCF7 or T47D breast cancer cells (Table 2). On the basis of previous studies, this signal was assigned to a choline-ether-phospholipid (26, 27), presumably 1-alkyl-2-acyl-*sn*-glycero-3-PCho (28).

In the ^{13}C spectra of the lipid phase extracts of MCF7 cells, we observed incorporation of the ^{13}C-enriched methylenes of choline into PtdCho (Fig. 5*A*), with no signs of their incorporation into other lipids. However, in the ^{13}C spectra of HMECs, unique ^{13}C methylene signals of nonenriched and [1,2-^{13}C]choline-enriched lipid were detected, in addition to the presence of ^{13}C-enriched PtdCho (Fig. 5*B*). We have tentatively assigned these signals to the choline-ether-phospholipid, detected exclusively in the ^{31}P spectra of HMECs. This assignment was based on: (*a*) a characteristic chemical shift; (*b*) $^{13}C_1$-$^{13}C_2$ splitting (40 Hz); (*c*) splitting attributable to the neighboring phosphate (5.1 Hz); and (*d*) similarity in the areas of the signals (~10% of PtdCho) in ^{31}P and ^{13}C spectra.

Quantitative analysis of the signals in the ^{31}P and ^{13}C spectra indicated similarities in the extent of ^{13}C labeling of PtdCho in the cancer and normal cells (39 ± 2% and 33 ± 5%, respectively; mean ± SD). Thus, although transport and phosphorylation of choline were faster in the cancer cells, the turnover of PtdCho appeared to proceed at about the same rate in both the normal and cancer cells, indicating similar control of the rate-limiting, cytosine-diphosphocholine synthesis. The extent of ^{13}C labeling of the unique HMEC choline-ether-phospholipid (11 ± 3%) was of the same order of magnitude as that of PtdCho, indicating continuous, significant incorporation of choline into both phospholipids. This finding suggests that this unique lipid plays an important role in the normal functioning of mammary cells.

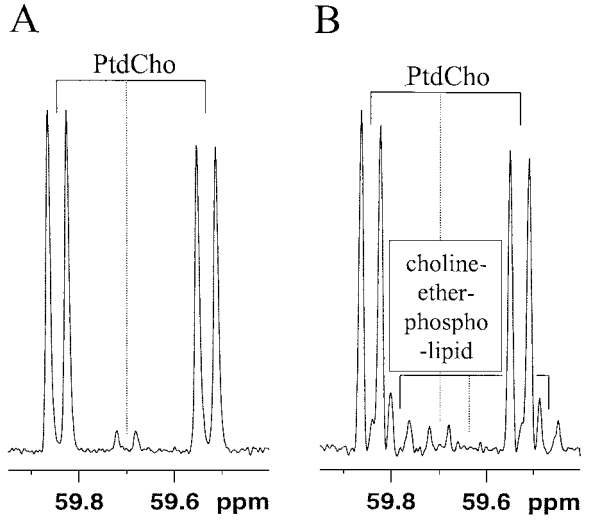

Fig. 5. ^{13}C spectra in the region of $^{13}C_1$ of choline-phospholipids of the lipid phase of MCF7 and HMEC cell extracts. MCF7 cells (*A*) and HMECs (*B*) were incubated with [1,2-^{13}C]choline as described in "Materials and Methods." The *solid lines* mark the signals of the [1,2-^{13}C]-labeled phospholipids, and the *dotted lines* mark the signals of the phospholipids at natural abundance. The spectra were acquired with 11,100 scans (*A*) and 19,700 scans (*B*).

A substantial difference was found in the levels of the ethanolamine-ether-phospholipid phosphatidylethanolamine plasmalogen in the normal cells and in the cancer cells (Table 2). It was thus concluded that the capacity of normal mammary cells to synthesize ether-phospholipids was markedly suppressed in their malignant counterpart.

DISCUSSION

In this study, we focused on investigating alterations in choline transport, oxidation, and phosphorylation induced by malignant transformation of HMECs. In addition, we searched for differences in membrane phospholipid composition and choline incorporation into those lipids in normal and cancerous mammary cells.

A sensitive radioactive labeling method and detailed measurements taken to determine the kinetic parameters of choline transport demonstrated the presence of both a saturable and a nonsaturable transport mechanism with significantly different rate parameters. The maximum rate of the saturable component of choline transport was >2-fold faster in the cancer cells, whereas the diffusion rate constant was higher in the normal cells (Table 1). The saturable mechanism predominated in the physiological range of choline in human plasma. It is therefore reasonable to propose that, in breast cancer patients, choline uptake into a malignant lesion is faster than its uptake into the surrounding normal glandular tissue. In addition, the increased choline kinase activity demonstrated in transformed cells (29) may further augment the level of PCho in these cells, thus increasing further the intensity of the composite choline signal of breast cancer, as recorded by MRS, to detectable levels.

Choline uptake into mammary epithelial cells was investigated previously in cells isolated from lactating rats (30). In the rat lactating cells, as in HMECs, saturable and nonsaturable mechanisms were found to be operative, with the former predominating at physiological concentrations (30). The mean K_m of the saturable component (35 ± 16 μM) was within the range of that found here for HMECs and MCF7 cells (Table 1). However, the V_{max} of transport (1.24 ± 0.19 nmol/mg protein/h) was lower, presumably because of differences in species and isolation protocols.

The nonsaturable transport in HMECs and MCF7 cells contributed to the uptake at high external choline concentrations and presumably occurred via passive diffusion, as was also suggested for the lactating rat mammary cells (30).

The phospholipid distribution of both normal HMECs and MCF7 human breast cancer cells revealed similarities in composition of diacyl phospholipids and sphingomyelin but pointed up a substantial decrease in the amount of the ether-phospholipids in the cancer cells. Levels of both choline-ether-phospholipids and ethanolamine-ether-phospholipids were significantly lower in the cancer cells relative to HMECs and to amounts detected in mammary fibroblasts (Ref. 17;

data not shown). The role played by ether phospholipids in mammary cells is currently unclear. Furthermore, it is also not known how a lack of these phospholipids might affect breast cancer etiology, despite interest in the function of ether lipids in cancer therapy (31). However, it appears reasonable to propose that the enhanced rates of passive diffusion of the positively charged choline through the cell membranes of HMECs, relative to that of MCF7, could be associated with the unique alterations in the phospholipid subclasses making up the membrane. In addition, our novel finding that human breast cancer cells contain reduced amounts of ether phospholipids might be related to the differential anticancer activity of alkyl-lysophospholipids (31), which in turn is associated with disturbances in membrane phospholipid metabolism (32–36).

In this study, we confirmed that most of the choline in MCF7 cells was converted to PCho and then routed through the cytosine-diphosphocholine pathway to form choline phospholipids (21, 37). In addition, we showed that a significant amount of choline (~25%) was oxidized to betaine, and most of it was found in the growth medium of the cells. It therefore appears that the two non-intersecting pathways, phosphorylation and oxidation of choline, are augmented in the course of malignant transformation of mammary cells.

In summary, our results demonstrated enhanced transport of choline, an augmented synthesis of PCho and betaine, and a unique suppression of the synthesis of choline-derived ether lipids in MCF7 and T47D human breast cancer cells. These biochemical changes support the diagnostic utilization of the composite choline magnetic resonance signal as a marker for breast cancer.

ACKNOWLEDGMENTS

We thank Barbara Morgenstern for editing the manuscript.

REFERENCES

1. Negendank, W. Studies of human tumors by MRS: a review. NMR Biomed., *5:* 303–324, 1992.
2. Preul, M. C., Caramanos, Z., Collins, D. L., Villemure, J. G., Leblanc, R., Olivier, A., Pokrupa, R., and Arnold, D. L. Accurate, noninvasive diagnosis of human brain tumors by using proton magnetic resonance spectroscopy. Nat. Med., *2:* 323–325, 1996.
3. Cecil, K. M., Schnall, M. D., Siegelman, E. S., and Lenkinski, R. E. The evaluation of human breast lesions with magnetic resonance imaging and proton magnetic resonance spectroscopy. Breast Cancer Res. Treat., *68:* 45–54, 2001.
4. Roebuck, J. R., Cecil, K. M., Schnall, M. D., and Lenkinski, R. E. Human breast lesions: characterization with proton MR spectroscopy. Radiology, *209:* 269–275, 1998.
5. Yeung, D. K., Cheung, H. S., and Tse, G. M. Human breast lesions: characterization with contrast-enhanced *in vivo* proton MR spectroscopy—initial results. Radiology, *220:* 40–46, 2001.
6. Gribbestad, I. S., Singstad, T. E., Nilsen, G., Fjosne, H. E., Engan, T., Haugen, O. A., and Rinck, P. A. *In vivo* ^{1}H MRS of normal breast and breast tumors using a dedicated double breast coil. J. Magn. Reson. Imag., *8:* 1191–1197, 1998.
7. Kvistad, K. A., Bakken, I. J., Gribbestad, I. S., Ehrnholm, B., Lundgren, S., Fjosne, H. E., and Haraldseth, O. Characterization of neoplastic and normal human breast tissues with *in vivo* ^{1}H MR spectroscopy. J. Magn. Reson. Imag., *10:* 159–164, 1999.
8. Jagannathan, N. R., Kumar, M., Seenu, V., Coshic, O., Dwivedi, S. N., Julka, P. K., Srivastava, A., and Rath, G. K. Evaluation of total choline from *in-vivo* volume localized proton MR spectroscopy and its response to neoadjuvant chemotherapy in locally advanced breast cancer. Br. J. Cancer, *84:* 1016–1022, 2001.
9. Zeisel, S. H., Costa, K. A. D., Franklin, P. D., Alexander, E. A., Lamont, J. T., Sheard, N. F., and Beiser, A. Choline, an essential nutrient for humans. FASEB J., *5:* 2093–2098, 1991.
10. Blusztajn, J. K. Choline, a vital amine. Science (Wash. DC), *281:* 794–795, 1998.
11. Rohlfs, E. M., Garner, S. C., Mar, M. H., and Zeisel, S. H. Glycerophosphocholine and phosphocholine are the major choline metabolites in rat milk. J. Nutr., *123:* 1762–1768, 1993.
12. Katz-Brull, R., Margalit, R., and Degani, H. Differential routing of choline in implanted breast cancer and normal organs. Magn. Reson. Med., *46:* 31–38, 2001.
13. Aboagye, E. O., and Bhujwalla, Z. M. Malignant transformation alters membrane choline phospholipid metabolism of human mammary epithelial cells. Cancer Res., *59:* 80–84, 1999.
14. Exton, J. H. Signaling through phosphatidylcholine breakdown. J. Biol. Chem., *265:* 1–4, 1990.
15. Pelech, S. L., and Vance, D. E. Signal transduction via phosphatidylcholine cycles. Trends Biochem. Sci., *14:* 28–30, 1989.
16. Singer, S., Souza, K., and Thilly, W. G. Pyruvate utilization, phosphocholine and adenosine triphosphate (ATP) are markers of human breast tumor progression: a ^{31}P and ^{13}C-nuclear magnetic resonance (NMR) spectroscopy study. Cancer Res., *55:* 5140–5145, 1995.
17. Ting, Y. T., Sherr, D., and Degani, H. Variations in the energy and phospholipid metabolism in normal and cancer human mammary epithelial cells. Anticancer Res., *16:* 1381–1388, 1996.
18. Ronen, S. M., and Leach, M. O. Imaging biochemistry: applications to breast cancer. Breast Cancer Res., *3:* 36–40, 2001.
19. Hernandez-Alcoceba, R., Saniger, L., Campos, J., Nunez, M. C., Khaless, F., Gallo, M. A., Espinosa, A., and Lacal, J. C. Choline kinase inhibitors as a novel approach for antiproliferative drug design. Oncogene, *15:* 2289–2301, 1997.
20. Hernandez-Alcoceba, R., Fernandez, F., and Lacal, J. C. *In vivo* antitumor activity of choline kinase inhibitors: a novel target for anticancer drug discovery. Cancer Res., *59:* 3112–3118, 1999.
21. Katz-Brull, R., and Degani, H. Kinetics of choline transport and phosphorylation in human breast cancer cells; NMR application of the zero trans method. Anticancer Res., *16:* 1375–1380, 1996.
22. Bradford, M. M. A rapid and sensitive method for the quantitation of microgram quantities of protein utilizing the principle of protein-dye binding. Anal. Biochem., *72:* 248–254, 1976.
23. Stein, W. D. Kinetics of transport: analyzing, testing and characterizing models using kinetic approach. Methods Enzymol. Biomembr., *171:* 23–62, 1989.
24. Tyagi, R. K., Azrad, A., Degani, H., and Salomon, Y. Simultaneous extraction of cellular lipids and water-soluble metabolites: evaluation by NMR spectroscopy. Magn. Reson. Med., *35:* 194–200, 1996.
25. Meneses, P., and Glonek, T. High resolution ^{31}P NMR of extracted phospholipids. J. Lipid Res., *29:* 679–689, 1988.
26. Merchant, T. E., Meneses, P., Gierke, L. W., Den Otter, W., and Glonek, T. ^{31}P magnetic resonance phospholipid profiles of neoplastic human breast tissues. Br. J. Cancer, *63:* 693–698, 1991.
27. Merchant, T. E., Characiejus, D., Kasimos, J. N., Den Otter, W., Gierke, L. W., and Glonek, T. Phosphodiesters in saponified extracts of human breast and colon tumors using ^{31}P magnetic resonance spectroscopy. Magn. Reson. Med., *26:* 132–140, 1992.
28. Street, J. C., and Koutcher, J. A. Effect of radiotherapy and chemotherapy on composition of tumor membrane phospholipids. Lipids, *32:* 45–49, 1997.
29. Ishidate, K. Choline/ethanolamine kinase from mammalian tissues. Biochim. Biophys. Acta, *1348:* 70–78, 1997.
30. Chao, C. K., Pomfret, E. A., and Zeisel, S. H. Uptake of choline by rat mammary-gland epithelial cells. Biochem. J., *254:* 33–38, 1988.
31. Ruiter, G. A., Verheij, M., Zerp, S. F., and van Blitterswijk, W. J. Alkyl-lysophospholipids as anticancer agents and enhancers of radiation-induced apoptosis. Int. J. Radiat. Oncol. Biol. Phys., *49:* 415–419, 2001.
32. Modolell, M., Andreesen, R., Pahlke, W., Brugger, U., and Munder, P. G. Disturbance of phospholipid metabolism during the selective destruction of tumor cells induced by alkyl-lysophospholipids. Cancer Res., *39:* 4681–4686, 1979.
33. Herrmann, D. B. Changes in cellular lipid synthesis of normal and neoplastic cells during cytolysis induced by alkyl lysophospholipid analogues. J. Natl. Cancer Inst., *75:* 423–430, 1985.
34. Wieder, T., Geilen, C. C., and Reutter, W. Antagonism of phorbol-ester-stimulated phosphatidylcholine biosynthesis by the phospholipid analogue hexadecylphosphocholine. Biochem. J., *291:* 561–567, 1993.
35. Boggs, K. P., Rock, C. O., and Jackowski, S. Lysophosphatidylcholine attenuates the cytotoxic effects of the antineoplastic phospholipid 1-*O*-octadecyl-2-*O*-methyl-rac-glycero-3-phosphocholine. J. Biol. Chem., *270:* 11612–11618, 1995.
36. Posse de Chaves, E., Vance, D. E., Campenot, R. B., and Vance, J. E. Alkylphosphocholines inhibit choline uptake and phosphatidylcholine biosynthesis in rat sympathetic neurons and impair axonal extension. Biochem. J., *312:* 411–417, 1995.
37. Katz-Brull, R., Bendel, P., Margalit, R., and Degani, H. Choline metabolism in breast cancer: ^{2}H, ^{13}C & ^{31}P NMR studies of cells and tumors. MAGMA, *6:* 44–52, 1998.